



OPEN ACCESS

EDITED BY
Buyun Du,
Jiangsu Open University, China

REVIEWED BY
Yongbing Cai,
Anhui Science and Technology
University, China
Wei Liu,
China University of Geosciences
Wuhan, China
Yuchuan Sun,
Southwest University, China

*CORRESPONDENCE
Wei Li,
liweili210@126.com

SPECIALTY SECTION
This article was submitted to
Toxicology, Pollution and the
Environment,
a section of the journal
Frontiers in Environmental Science

RECEIVED 10 July 2022
ACCEPTED 21 July 2022
PUBLISHED 05 September 2022

CITATION
An X, Li W, Lan J, Di X and Adnan M
(2022), Seasonal co-pollution
characteristics of parent-PAHs and
alkylated-PAHs in karst mining area soil
of Guizhou, Southwest China.
Front. Environ. Sci. 10:990471.
doi: 10.3389/fenvs.2022.990471

COPYRIGHT
© 2022 An, Li, Lan, Di and Adnan. This is
an open-access article distributed
under the terms of the [Creative
Commons Attribution License \(CC BY\)](https://creativecommons.org/licenses/by/4.0/).
The use, distribution or reproduction in
other forums is permitted, provided the
original author(s) and the copyright
owner(s) are credited and that the
original publication in this journal is
cited, in accordance with accepted
academic practice. No use, distribution
or reproduction is permitted which does
not comply with these terms.

Seasonal co-pollution characteristics of parent-PAHs and alkylated-PAHs in karst mining area soil of Guizhou, Southwest China

Xianjin An ^{1,2†}, Wei Li^{3*}, Jiacheng Lan^{1,2}, Xinyue Di⁴ and Muhammad Adnan^{5,6}

¹School of Karst Science, Guizhou Normal University, Guiyang, China, ²State Engineering Technology Institute for Karst Desertification Control, Guiyang, China, ³College of Biology and Environmental Engineering, Guiyang University, Guiyang, China, ⁴School of Geography and Environmental Engineering, Gannan Normal University, Ganzhou, China, ⁵State Key Laboratory of Environmental Geochemistry, Institute of Geochemistry, Chinese Academy of Sciences, Guiyang, China, ⁶University of Chinese Academy of Sciences, Beijing, China

The research on polycyclic aromatic hydrocarbons (PAHs) in karst soil mainly focuses on 16 kinds of parent-PAHs (p-PAHs), and little attention is given to alkylated-PAHs (a-PAHs) with higher concentration and greater toxicity. Five surface soils of coal mining area and their surrounding areas in karst area were sampled as subject investigated, and the spatiotemporal pollution characteristics of p-PAHs and a-PAHs were analyzed to discuss the impact of karst soil properties and environmental conditions on the migration of a-PAHs. The research results showed that the pollution concentration of a-PAHs in the soil of the southwestern karst area, especially the coal mining area, was significantly higher compared to the 16 kinds of p-PAHs, and the average concentration of the p-PAHs was 177.29 ± 37.36 ng/g; the concentration of a-PAHs was 346.87 ± 104.91 ng/g; the concentration of PAHs presented a seasonal pattern of that in winter > spring > autumn > summer. At the same time, seasonal rainfall could affect and change the occurrence state of PAHs in karst soils, but the effect on p-PAHs was weaker than on a-PAHs. The concentration of PAHs in the coal mining area and forest soil were 651.68 ng/g and 755.38 ng/g, respectively, so they belonged to contaminated soil, while the concentrations of two cultivated soil and abandoned soil were 475.51 ng/g, 367.58 ng/g and 370.63 ng/g, respectively, belonging to weakly contaminated. Toxicity assessment showed that p-BaP with a maximum toxic equivalent of 62.35 ng/g, C₁-BaP (42.09 ng/g), DaA (37.82 ng/g) and C₁₋₃ BaA (25.91 ng/g) were toxic PAHs with higher risk. The results of the correlation study showed that soil organic carbon, soil clay and soil calcium content were the dominant factors affecting the spatiotemporal distribution of PAHs of soils in karst coal mining areas and their surrounding areas. The research can provide data guidance for the management, control and restoration of soil pollution in karst areas, and offer a reference for Guizhou province to implement the big-ecological strategy.

KEYWORDS

karst, soil, parent-PAHs, alkylated-PAHs, seasonal variations, pollution characteristics

Introduction

Global karst landforms were widely distributed, accounting for about 15% of the terrestrial area (Larson and Mylroie, 2018). Guizhou province was China's distribution center of karst landforms (Yan et al., 2019). Karst areas are vulnerable to various exogenous pollutants due to their extremely fragile ecosystems and thin soil layers. The coal-dominated energy consumption structure, rapid urbanization, and the increasing number of motor vehicles have made Guizhou province karst soil a major "sink" of PAHs. Research pointed out that the total emission of PAHs was 1730 tons in Guizhou province, ranking fourth in the country in 2003 (Xu et al., 2006), and Guizhou province's overall emission intensity was also at a high level in China (Zhang et al., 2007). Han et al. (2019) pointed out that China emitted 32,700 tons of PAHs because of incomplete fuel combustion in 2016, and the emission intensity of Guizhou province was high. Zhang et al. (2022) pointed out that the pollutant concentration of soil PAHs near the coal-fired power plant in the karst area of Guizhou province reached 12.2 mg/kg.

The occurrence, migration and fate of 16 kinds of p-PAHs in the environmental priority control pollutants in soil have been widely studied, but the total polycyclic aromatic compounds (PACs) in the environment not only contain 16 kinds of p-PAHs, but also include a-PAHs, nitro-polycyclic aromatic hydrocarbons (n-PAHs), dibenzothiophenes (DBTs), etc. In recent years, researchers have found that aerosols (Wei et al., 2015), bituminous coal (Zhang et al., 2021), coking plants and coal gangue (Lin et al., 2017; Liang et al., 2018), oil-contaminated sites (Golzadeh et al., 2021), untreated sludge and municipal wastewater (Hellou et al., 1999) include not only 16 kinds of p-PAHs, but also a large number of a-PAHs whose proportion was often greater than p-PAHs. The main sources of a-PAHs included the accompanying products of petroleum, namely diagenetic sources; a-PAHs also existed in raw coal; the processing and combustion of petroleum and coal products also released a part of a-PAHs. The substitution reaction of p-PAHs in the environment also increased the concentration of a-PAHs in the environment. Studies have found that a-PAHs may be significantly more toxic than p-PAHs (Andersson and Achten 2015; Golzadeh et al., 2021). The study believed that PAHs with a "Bay region" structure was the key molecular feature that affected whether PAHs would lead to mutagenesis, carcinogenesis and teratogenesis. The study also found that 38 kinds of a-PAHs had the above three effects (Baird et al., 2007).

The climate, precipitation and various Earth surface processes in southwest China's karsts were extremely complicated, which may affect PAHs' environmental migration and final fate. Lan et al. (2016, 2018) showed that rainfall events changed the distribution of PAHs in karst groundwater, the mass concentration of PAHs in water

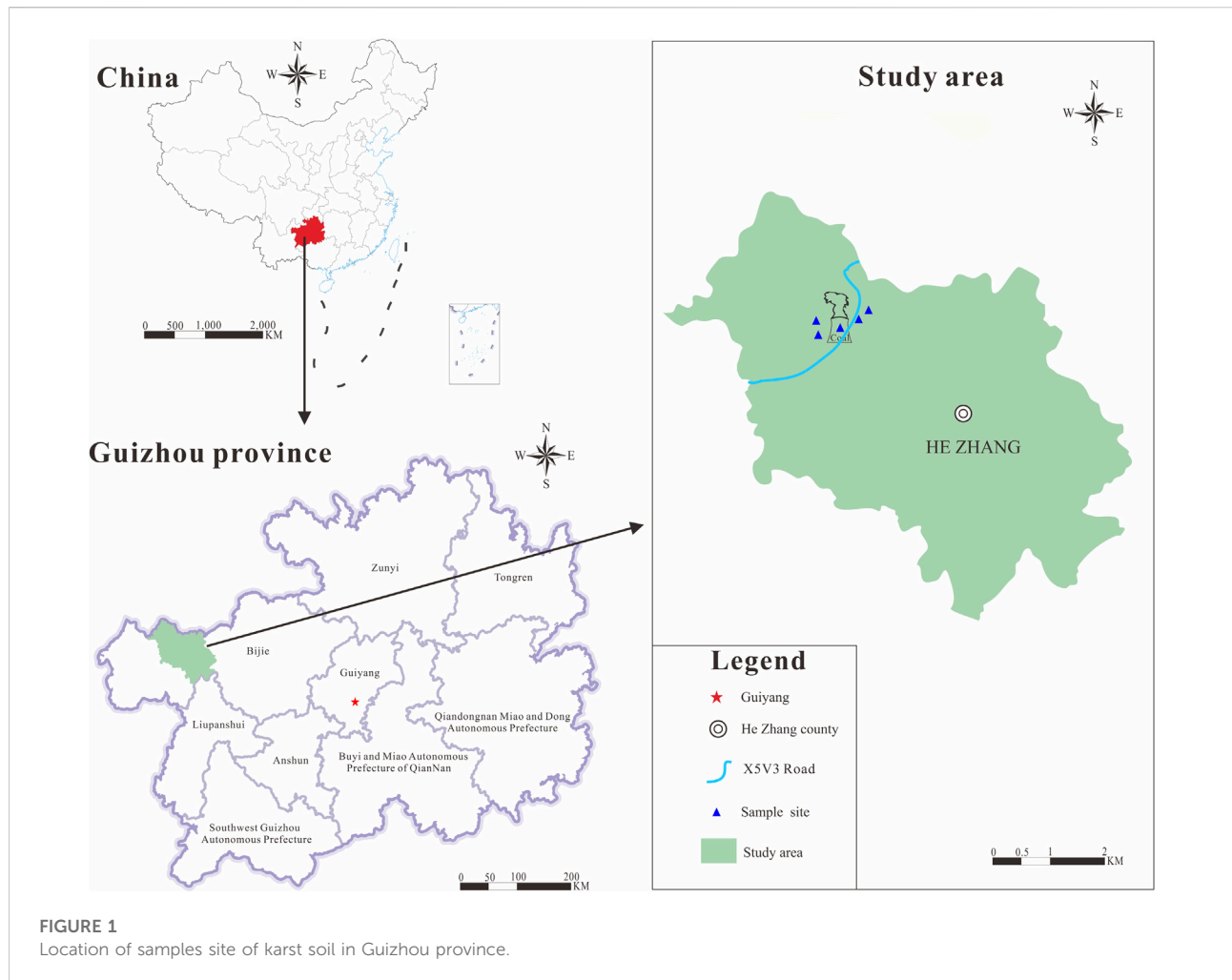
increased with the increase of rainfall or flow, and the ecological risk of underground water changed during rainfall. Zhu et al. (2022) showed that high ring PAHs were more enriched in the soil of typical karst trough valleys in Chongqing, and soil PAHs generally caused a low risk of carcinogenicity. Qian et al. (2020) showed that low cyclic PAH was mainly found in the karst cave sediment, and PAHs distribution had no significant relationship with the sediment particle size. Ye et al. (2015) believed that the migration of PAHs in karst areas was mainly controlled by two mechanisms: organic matter and water dissolution. They believed that energy combustion and traffic pollution, and atmospheric deposition were the main pollution pathway for PAHs in the study area. An et al. (2021) believed that the migration of PAHs in karst soil was closely related to natural ecological processes such as freezing and thawing. Freeze-thaw cycles may affect the form of calcium ions in the karst environment, thereby changing the microscopic morphology and structure of soil organic matter, resulting in changes in PAHs occurrence state and desorption process. The research on PAHs in the karst environment mainly focused on groundwater and 16 kinds of p-PAHs, while the more toxic a-PAHs and 16 kinds of p-PAHs in soil had not been reported.

Meanwhile, the physicochemical properties of a-PAHs and p-PAHs were quite different, which may affect the occurrence, migration and toxicity in the environment (Kang et al., 2016). The pollution of a-PAHs in southwestern karst areas, especially in coal-rich areas, would inevitably affect soil health and groundwater safety, and ultimately affected the safety of the entire regional ecosystem and human health. In addition, the unique climatic conditions in the karst area of Guizhou province may change the occurrence and migration of p-PAHs and a-PAHs. Hence, studying the pollution characteristics of a-PAHs in karst areas was necessary. The main purpose of this study was to find out the temporal and spatial distribution tendency of PAHs in the soil of karst coal-rich areas in different seasons, analyze the possible influencing factors, calculate the ecological risk value. The research can provide data guidance for the management, control and restoration of soil pollution in karst areas, and provide a reference for implementing the big ecology strategy in Guizhou province.

Material and methods

Sample collection

The study selected five surface soils (0–10 cm) in a coal mining area in Hezhang County, Guizhou province (Figure 1). The coal mining area was 2.29 km², and the production scale was



0.45 Mt/a. The coal-bearing formation of the coal mine was Xuanwei Group (P3x), which mainly was lignite with medium high sulfur and low volatile anthracite. The study was conducted in March, 2021 (spring, with continuous light rain for a week before sampling), June, 2021 (summer, with a heavy rain for a week before sampling), September, 2021 (autumn, without rainfall for a week before sampling), and December, 2021 (winter, without rainfall for a week before sampling). 10 m × 10 m surface soil mixed sample was collected by the W-type sampling method, which was air-dried at room temperature in the laboratory in the dark to remove plant roots and debris, ground and screened through a 100-mesh stainless steel sieve, and put in a sealed bag for later use. The basic characteristics of the soil are shown in Table 1. The total organic carbon (TOC) was measured by an organic element analyzer (vario Macro cube), and the cation exchange capacity (CEC) was measured by the $\text{NH}_4\text{Cl-NH}_4\text{OAc}$ method. The total calcium amount of the

soil (TCA) was digested using aqua regia-perchloric acid and determined by the ICP-OES method. Soil texture was determined using a laser particle size analyzer (BT-9300ST).

Instruments and reagents

The main experimental apparatus included Agilent 6890/5973B gas chromatography-mass spectrometer (equipped with EI ionization source and automatic sampler); rotary evaporator (VORTEX-5), ultrasonic cleaner (KG-250DE type), centrifuge (TGL -16C).

N-hexane and dichloromethane were products of Thermal Fisher, the United States; methanol and anhydrous sodium sulfate were bought from Sinopharm Group Corporation. The standard mixed samples of 16 kinds of p-PAHs were purchased from AccuStandard, the United States, and the standard

TABLE 1 Physical and chemical properties of the soil at the sampling sites.

Sample	pH	TOC (%)	CEC (cmol/kg)	TCA (10 ⁻³ cmol/kg)	Soil texture(%)			Descriptions
					Silt	Clay	Sand	
S1	6.39	3.55	11.28	5.21	33.26	20.23	46.51	The soil in the mining area, without the vegetation
S2	7.62	3.84	23.57	3.22	19.24	43.92	36.84	Abandoned soil, with horsetail pine
S3	7.48	5.61	12.28	4.38	11.36	67.06	21.58	Slope soil, perennial planting pepper
S4	7.24	4.47	14.57	3.47	40.29	24.54	35.17	Cultivated soil, mainly planting corn
S5	7.37	9.46	26.45	6.35	26.48	39.03	34.49	Forest soil

solutions of 12 a-PAHs were purchased from Ehrenstorfer, Germany. Preprocessing standard internal D₈-naphthalene, quantitative internal standard D₁₀-acenaphthene, D₁₀-phenanthrene, D₁₂-perylene, D₁₂-chrysen, and injection internal standard D₁₄-tribiphenyl were purchased from Cambridge Isotope Laboratories.

Extraction and analysis

Ultrasonic extraction was used to extract the p-PAHs and a-PAHs in the soil. Briefly, 5 g sample was put into a 10 ml screw-top glass test tube, then 2 g high-temperature treated anhydrous sodium sulfate was added, then 100 μ L with 20 μ g/ml recovery internal standard D₈-naphthalene was added, and meanwhile 10 ml of dichloromethane was added. At a constant water temperature of 20°C, the sample was sonicated for 5 h, and stirred once per hour during ultrasonication. The supernatant was transferred to a centrifuge tube, centrifuged at 14,000 r/min for 5 min, and then transferred to a rotary evaporator, which was concentrated to 0.5 ml, transferred to a 1.5 ml brown injection bottle. 100 μ L with 400 ng/g quantitative internal standard (D₁₀-acenaphthene, D₁₀-phenanthrene, and D₁₂-perylene) was added. The sample capacity was fixed to 1 ml using methanol, and evenly was mixed in a vortexer for 5 min to tested on the machine.

The sample was measured by GC-MS, and the specific chromatographic parameters were as follows: temperature programming of the chromatographic column (DB-5MS, 30 m \times 0.25 mm \times 0.25 μ m, United States) started from 70°C, and held for 1 min; the chromatographic column was heated to 180°C at 15°C/min, held for 2 min; heated to 220°C at 10°C/min, held for 0.5 min, and finally heated to 300°C at 8°C/min, held for 5 min. The carrier gas was helium, the flow rate was constant flow with 1.0 ml/min; the injection port temperature was 280°C, and the injection volume was 1 μ L without split sampling. Mass spectrometry parameters: electron bombardment ion source, ionization voltage 70 eV, ion source temperature 230°C, interface temperature 280°C, mass scanning range m/z 50–550, in full scan mode, solvent delay for 4 min.

Data processing and quality control

The p-PAHs were determined by gas chromatography-mass spectrometry, specifically referred to by Lan et al. (2016). The a-PAHs were qualitatively and quantitatively analyzed using MassLynx V4.2 software by referring to the mass spectrum of the standard sample and the mass spectrum in the standard mass spectrum database (NIST Mass Spectral Database), and qualitative analysis was made based on retention time. The relative response factor (RF) internal standard method was used for quantitative analysis; the components of a-PAHs not included in the standard sample were quantified according to the response factors of PAHs or a-PAHs with the closest retention time in the homologues or the chromatogram (Qian et al., 2022). The RF calculation formula was as follows:

$$RF = \frac{K_{S-PAH}}{K_{IS}} \quad (1)$$

In Eq. 1, K_{S-PAH} was the regression curve slope of a single PAH standard substance; K_{IS} was the regression curve slope of the added standard internal substance corresponding to a single PAH standard substance.

All samples were subject to a strict quality assurance and quality control system: 3 parallel samples were set for each sample, and the recovery standard sample was added; the actual recovery ranges were D₈-naphthalene (83.2% \pm 6.3%), D₁₀-Acenaphthene (79.2% \pm 8.4%), D₁₀-phenanthrene (95.1% \pm 2.8%), D₁₂-chrysen (98.2% \pm 3.4%), D₁₂-perylene (102.6% \pm 6.5%); one blank was added for every 10 samples, and the concentration range of naphthalene was 0.03–0.95 ng/g in the blank sample; the final data were revised from the blank and corrected for recovery.

Results

Concentration characteristics of Σ PACs

35 kinds of PACs (14 kinds of p-PAHs and 21 kinds of a-PAHs) were detected in the samples, and the concentrations of 14 kinds of p-PAHs ranged from 224.66 \pm 55.78 ng/g to

TABLE 2 Concentration of \sum_{16} p-PAHs in samples of soil (ng/g).

p-PAH	S1 ^a	S2	S3	S4	S5	Average
Nap	11.46 ± 1.17	5.26 ± 1.3	14.38 ± 1.42	4.95 ± 2.1	13.93 ± 3.97	9.99 ± 1.99
Acy	ND	ND	ND	ND	ND	ND
Ace	ND	ND	ND	ND	ND	ND
Flu	15.55 ± 2.13	11.25 ± 2.55	12.49 ± 3.83	10.74 ± 1.43	16.14 ± 2.48	13.23 ± 2.48
Phe	16.37 ± 2.42	8.72 ± 1.72	16.82 ± 3.11	9.6 ± 2.84	23.18 ± 3.46	14.93 ± 2.71
Ant	17.12 ± 1.77	10.39 ± 2.01	13.03 ± 2.27	10.36 ± 3.14	17.03 ± 2.98	13.59 ± 2.43
Fla	17.83 ± 2.62	12.51 ± 1.39	13.44 ± 2.71	11.46 ± 2.37	24.82 ± 5.19	16.01 ± 2.86
Pyr	23.47 ± 3.04	12.47 ± 2.48	17.27 ± 4.42	9.64 ± 1.64	16.73 ± 3.77	15.92 ± 3.07
BaA	12.33 ± 2.29	10.16 ± 1.57	11.7 ± 3.08	9.03 ± 1.09	16.99 ± 5.23	12.04 ± 2.65
Chr	11.06 ± 2.06	9.88 ± 1.84	12.89 ± 3.76	7.84 ± 1.69	18.6 ± 6.69	12.05 ± 3.21
BbF	19.39 ± 2.2	14.52 ± 2.31	20.42 ± 8.26	14.2 ± 1.29	27.92 ± 7.36	19.29 ± 4.28
BkF	6.47 ± 2.12	6.38 ± 3.06	11.41 ± 2.99	8.01 ± 1.98	10.31 ± 3.21	8.52 ± 2.67
BaP	14.15 ± 2.46	9.89 ± 2.06	15.2 ± 1.93	7.82 ± 2.13	15.3 ± 5.10	12.47 ± 2.73
DaA	13.2 ± 1.51	5.88 ± 1.35	13.18 ± 4.05	5.56 ± 2.43	ND	7.56 ± 1.87
InP	12.54 ± 1.06	7.13 ± 1.27	9.35 ± 2.95	5.28 ± 1.46	11.32 ± 3.26	9.12 ± 2.00
BgP	16.72 ± 1.62	12.25 ± 2.51	14.47 ± 3.5	6.97 ± 1.32	12.41 ± 3.09	12.56 ± 2.41
2–3 ring \sum PAHs	60.49 ± 7.48	35.61 ± 7.58	56.72 ± 10.62	35.63 ± 9.50	70.28 ± 12.89	51.75 ± 9.62
4 ring \sum PAHs	64.68 ± 10.01	45.02 ± 7.28	55.29 ± 13.97	37.96 ± 6.78	77.14 ± 20.88	56.02 ± 11.78
5–6 ring \sum PAHs	82.47 ± 10.95	56.05 ± 12.56	84.03 ± 23.68	47.84 ± 10.61	77.25 ± 22.02	69.52 ± 15.96
\sum PAHs	207.64 ± 28.45	136.67 ± 27.42	196.04 ± 48.27	121.43 ± 26.89	224.66 ± 55.78	177.29 ± 37.36

Note: ND was not detected (the same below).

^aIndicates the average concentration of samples at the same location in the four-sampling season. [Abbreviations: Nap, Naphthalene; Acy, Acenaphthylene; Ace, Acenaphthene; Flu, Fluorene; Phe, Phenanthrene; Ant, Anthracene; Fla, Fluoranthene; Pyr, Pyrene; BaA, Benzo(a)anthracene; Chr, Chrysene; BbF, Benzo(b)fluoranthene; BkF, Benzo(k)fluoranthene; BaP, Benzo(a)pyrene; DaA, Dibenzo(a,h)anthracene; InP, Indeno(1,2,3-cd)pyrene; BgP, Benzo(g,hi)perylene].

121.43 ± 26.89 ng/g, with an average value of 177.29 ± 37.36 ng/g; 21 kinds of a-PAHs concentrations ranged from 530.72 ± 172.17 ng/g to 444.04 ± 94.19 ng/g, with an average value of 346.87 ± 104.91 ng/g (Tables 2, 3). The two p-PAHs (acenaphthylene and acenaphthene) were not detected in the karst soil, but their alkyl-substituted hydrocarbons had high concentrations. According to analysis from the polluted site, the forest soil sampling site (S5) had the maximum concentration of p-PAHs (224.66 ± 66.82 ng/g), and the soil sampling site of traditional corn crop cultivated soil (S4) had the minimum value of p-PAHs (121.43 ± 31.94 ng/g). The specific concentration tendency was S5 > S1 > S3 > S2 > S4. Forest soil sampling site (S5) had the maximum concentration of the a-PAH (530.72 ± 172.17 ng/g), and cultivated corn crop soil (S4) still was the minimum value (249.21 ± 94.69 ng/g). The specific concentration tendency was S5 > S1 > S3 > S4 > S2. According to analysis from the sampling season: the average concentration of total PAHs in the five sampling sites was winter (588.01 ng/g) > spring (573.26 ng/g) > autumn (499.41 ng/g) > summer (435.95 ng/g). The average concentration of p-PAHs in the five sampling sites was winter (203.09 ± 41.65 ng/g) > autumn (177.56 ± 36.21 ng/g) > spring (169.31 ± 40.25 ng/g) > summer (159.18 ± 60.17 ng/g). Except for the winter in which the concentration of the S1 was higher than that of the other four

sampling sites, the concentration of the sampling site was exhibited with S5 > S1 > S3 > S2 > S4 in other seasons. However, there were differences in the seasonal distribution characteristics of a-PAHs. The seasonal distribution order of the five soil samples was spring (403.95 ± 41.65 ng/g) > winter (384.92 ± 113.38 ng/g) > autumn (321.85 ± 104.19 ng/g) > summer (276.77 ± 91.31 ng/g). Except for the spring sampling in which the content of a-PAHs in cultivated soil (S4) was lower than that in the abandoned soil (S2), the general trend of a-PAHs concentrations was S5 > S1 > S3 > S4 > S2 in the four seasons. A comparison of the concentration distribution of PAHs in different sites and in different sampling seasons with the soil properties of the sampling sites revealed that the spatial distribution of p-PAHs and a-PAHs were closely related to soil organic carbon content.

The \sum PACs in the mining area (S5) were significantly higher than in the other 4 sampling sites (Table 4); the p-PAHs concentration at all sampling sites was lower than the a-PAHs concentration. The a-PAHs accounted for 63%–70% of PACs, with an average value of 64%, which indicated that a-PAHs might be the main type of PAHs of the sampling sites surface soil in the karst area. In different seasons, the concentrations of PAHs in the soil were significantly different, with the total concentration of PAHs in the soil in winter and spring higher than that in autumn and summer.

TABLE 3 Concentration of Σ_{21} a-PAHs in samples of soil (ng/g).

a-PAH	CAS	S1	S2	S3	S4	S5	Average
1-Methylnaphthalene	90-12-0	25.64 ± 2.79	17.81 ± 2.09	22 ± 3.57	20.78 ± 2.35	24.33 ± 7.96	22.11 ± 3.75
2-Methylnaphthalene	91-57-6	21.92 ± 2.03	21.38 ± 1.52	22.1 ± 4.01	16.81 ± 1.72	31.59 ± 4.92	22.76 ± 2.84
2-Ethylnaphthalene	2949-26-0	7.83 ± 1.35	4.54 ± 4.43	5.74 ± 4.22	6.15 ± 4.23	11.58 ± 3.23	7.17 ± 3.49
2,7-Dimethylnaphthalene	582-16-1	24.22 ± 2.58	14.62 ± 1.92	13.74 ± 2.52	13.83 ± 2.17	25.33 ± 6.21	18.34 ± 3.08
2,3,5-Trimethylnaphthalene	2245-38-7	20.04 ± 4.33	10.8 ± 3.41	15.46 ± 4.46	13.56 ± 3.85	28.47 ± 10.99	17.66 ± 5.41
1-Methylfluorene	1730-37-6	25.93 ± 6.97	14.84 ± 3.15	16.17 ± 4.10	13.99 ± 3.56	27.74 ± 10.14	19.73 ± 5.59
9-Methylfluorene	2523-37-7	27.83 ± 7.95	11.07 ± 1.55	14.47 ± 3.36	13.87 ± 9.22	28.7 ± 4.99	19.19 ± 5.41
1,9-Dimethylfluorene	17057-98-6	22.96 ± 6.01	12.82 ± 4.47	16.75 ± 5.84	15.97 ± 5.05	34.82 ± 12.66	20.66 ± 6.81
1-Methylanthracene	610-48-0	29.97 ± 5.46	14.28 ± 4.07	14.15 ± 5.31	15.41 ± 4.60	53.5 ± 8.37	25.46 ± 5.56
2-Methylanthracene	613-12-7	27.52 ± 6.87	8.06 ± 1.01	10.44 ± 7.12	10.01 ± 6.53	21.07 ± 7.61	15.42 ± 5.83
9,10-Dimethylanthracene	781-43-1	23.93 ± 2.25	10.94 ± 2.82	14.3 ± 2.21	13.2 ± 3.18	28.85 ± 12.96	18.24 ± 4.68
2,9,10-Trimethylanthracene	63018-94-0	26.28 ± 5.05	10.4 ± 3.78	10.74 ± 4.92	7.89 ± 4.26	19.15 ± 9.66	14.89 ± 5.53
7-Methylbenz[a]anthracene	2541-69-7	20.78 ± 5.84	10.24 ± 4.36	13.36 ± 5.70	12.8 ± 4.92	26.97 ± 11.56	16.83 ± 6.47
12-Methylbenz[a]anthracene	2422-79-9	15.72 ± 1.74	12.44 ± 1.31	15.99 ± 12.56	14.52 ± 9.74	31.78 ± 13.22	18.09 ± 7.71
7,12-Dimethylbenz[a]anthracene	57-97-6	25.92 ± 3.57	9.57 ± 2.67	11.97 ± 3.52	11.94 ± 3.02	25.15 ± 8.61	16.91 ± 4.27
2-Methylphenanthrene	2531-84-2	22.12 ± 1.08	7.54 ± 3.66	10.79 ± 4.93	7.94 ± 7.87	25.97 ± 4.61	14.87 ± 4.43
9-Methylphenanthrene	883-20-5	14.16 ± 3.84	7.7 ± 2.86	9.25 ± 3.75	8.86 ± 3.24	18.65 ± 8.24	11.72 ± 4.39
4,5-Methylenphenanthrene	203-64-5	18.03 ± 8.99	3.79 ± 1.88	4.74 ± 3.8	5.19 ± 2.13	9.55 ± 4.99	8.26 ± 4.36
2,3,5-Trimethylphenanthrene	3674-73-5	12.7 ± 4.97	6.08 ± 3.71	7.79 ± 4.91	7.46 ± 4.19	15.72 ± 7.46	9.95 ± 5.05
1-Methylpyrene	3442-78-2	23.35 ± 3.90	16.3 ± 2.91	22.24 ± 3.81	12.04 ± 3.29	27.06 ± 5.88	20.2 ± 3.96
6-Methylbenzo[a]pyrene	2381-39-7	7.23 ± 6.64	5.73 ± 4.96	7.33 ± 6.45	7.02 ± 5.59	14.78 ± 7.95	8.42 ± 6.32
2 ring ΣA_{1-3} Nap ^a		99.64 ± 13.07	69.14 ± 13.37	79.03 ± 18.76	71.11 ± 14.31	121.29 ± 33.29	88.04 ± 18.56
3 ring ΣA_{1-3} Flu/Ant/Phe ^b		313.82 ± 70.59	139.75 ± 41.28	170.88 ± 71.97	159.04 ± 71.51	367.59 ± 125.05	230.22 ± 76.08
4–5 ring ΣA_{1-2} Pyr/BaA/BaP ^c		30.58 ± 10.54	22.03 ± 7.87	29.57 ± 10.26	19.06 ± 8.88	41.84 ± 13.84	28.62 ± 10.28
Σa -PAHs		444.04 ± 94.19	230.92 ± 62.52	279.48 ± 100.99	249.21 ± 94.69	530.72 ± 172.17	346.87 ± 104.91

^aMeans alkylated homologues of the 1-3 substituted of 2 ring naphthalene.

^bMeans alkylated homologues of the 1-3 substituted of 3 ring fluorene, fluorene and phenanthrene.

^cMeans alkylated homologues of the 1-2 substituted of 4–5 ring pyrene, benz[a]anthracene and benzo[a]pyrene.

TABLE 4 Distribution and ration of different kinds of PAHs content in sampling sites.

Sample	$\Sigma PACs$ (ng/g)	Σp -PAHs (ng/g)	Σa -PAHs (ng/g)	Ratio (a/p)	Ratio (p/ Σ)	Ratio (a/ Σ)
S1	651.68	207.64	444.04	2.14	0.32	0.68
S2	367.58	136.67	230.92	1.69	0.37	0.63
S3	475.51	196.04	279.48	1.43	0.41	0.59
S4	370.63	121.43	249.21	2.05	0.33	0.67
S5	755.38	224.66	530.72	2.36	0.30	0.70
Total	2620.78	886.43	1734.35	1.96	0.34	0.66

$\Sigma PACs$ pollution pattern

In all sampling sites, the a-PAHs were a significantly higher proportion than p-PAHs, and the proportion of a-PAHs accounted for 59%–70% of the total aromatic hydrocarbons. In terms of 16 kinds of p-PAHs, the concentration of 2–3-ring PAHs ranged from 35.61 ± 7.58 ng/g to 70.28 ± 12.89 ng/g, with

an average value of 51.75 ± 9.62 ng/g, accounting for 29.19%; the concentration of 4-ring p-PAHs ranged from 37.96 ± 6.78 ng/g to 77.14 ± 20.88 ng/g, with an average value of 56.02 ± 11.78 ng/g, accounting for 31.60%; the concentration of 5–6-ring p-PAHs ranged from 56.05 ± 12.56 ng/g to 84.03 ± 23.68 ng/g, with an average value of 69.52 ± 15.96 ng/g, accounting for 39.21%. The 2-ring a-PAHs had the highest value of 121.29 ± 33.29 ng/g in the

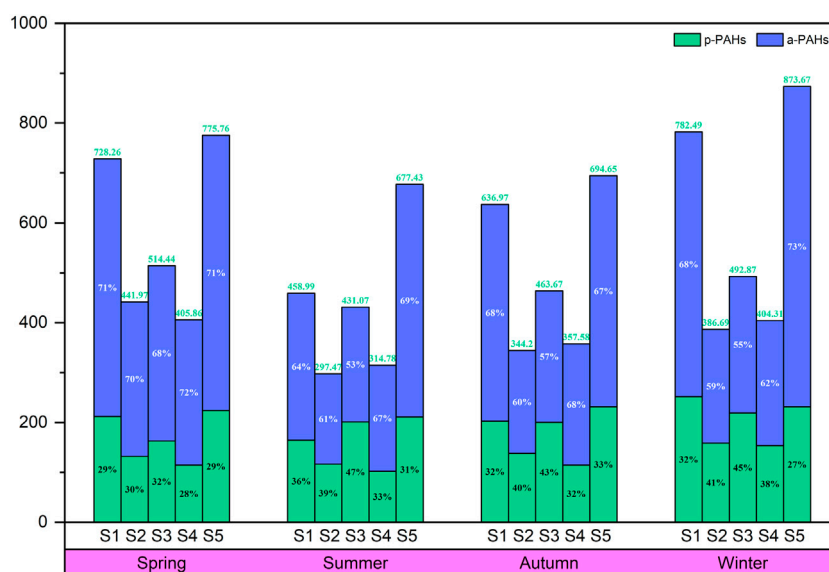


FIGURE 2
Distribution of p-PAHs and a-PAH in karst soils for different seasons.

S5 and the lowest value of 69.14 ± 13.37 ng/g in the S2, with an average value of 88.04 ± 18.56 ng/g, accounting for 25.38%. The 3-ring a-PAHs had the highest value of 367.59 ± 125.05 ng/g in the S5 and the lowest value of 139.75 ± 41.28 ng/g in the S2, with an average value of 230.22 ± 76.08 ng/g, accounting for 66.37%. The 4–5-ring a-PAHs had the highest value of 41.84 ± 13.84 ng/g in the S5 and the lowest value of 19.06 ± 8.88 ng/g in the S4, with an average value of 28.62 ± 10.28 ng/g, accounting for 8.25%.

Seen from the analysis of different sampling seasons (Figures 2, 3), the average concentrations of 2–3-ring p-PAHs were 47.27 ± 7.10 ng/g (spring), 46.97 ± 9.37 ng/g (summer), 54.38 ± 6.99 ng/g (autumn) and 58.36 ± 8.60 ng/g (winter); the average concentrations of 4-ring p-PAHs were 59.18 ± 13.04 ng/g (spring), 50.89 ± 22.75 ng/g (summer), 54.68 ± 11.22 ng/g (autumn) and 59.33 ± 11.90 ng/g (winter); the average concentrations of 5–6-ring p-PAHs were 62.86 ± 12.33 ng/g (spring), 61.32 ± 17.36 ng/g (summer), 68.51 ± 10.86 ng/g (autumn) and 85.40 ± 12.65 ng/g (winter). The average concentrations of 2-ring a-PAHs in spring, summer, autumn, and winter were 116.70 ± 20.66 ng/g, 57.47 ± 16.23 ng/g, 95.39 ± 19.93 ng/g, and 82.63 ± 17.42 ng/g, respectively; the average concentrations of 3-ring a-PAHs in spring, summer, autumn, and winter were 250.15 ± 79.98 ng/g, 193.58 ± 66.12 ng/g, 194.24 ± 74.46 ng/g, and 282.89 ± 83.74 ng/g, respectively. The average concentrations of 4–5-ring a-PAHs were 37.10 ± 10.12 ng/g in spring, 25.72 ± 8.96 ng/g in summer, 32.25 ± 9.80 ng/g in autumn, and 19.39 ± 12.22 ng/g in winter, respectively. As seen from the analysis of a-PAHs homologs

of the same type, the concentration of alkylated-naphthalene and alkylated-anthracene homologs were significantly higher than that of other a-PAHs homologs, while alkylated-BaP homologs had the smallest concentration and proportion (Figure 4). The 4–5-ring p-PAHs was a relatively high proportion, and there was a small difference between p-PAHs with different ring numbers, with a maximum value of 50.44% in winter. The a-PAHs with different ring numbers varied significantly, and the 3-ring a-PAHs were significantly higher proportion than 2-ring and 4–5-ring, and the largest proportion was 70.03% in winter.

Polycyclic aromatic compounds risk assessment

The soil PAHs pollution standard (Maliszewska-Kordybach 1996) was combined with the substance toxicity equivalent factor (Table 5) to evaluate the toxic concentration of p-PAHs and a-PAHs in the coal mining area and then conduct a risk assessment of the sample site in the coal area (Figure 5). The results showed that when only 16 kinds of p-PAHs were considered, except that the average concentration of the S5 ($0.22 \mu\text{g/g}$) and the average concentration of the S1 ($0.21 \mu\text{g/g}$) were slight pollutions, the samples of other sites were all non-pollution (Figure 5B). The concentration of a-PAHs in different sites and seasons was significantly higher than that of p-PAHs, and the pollution level was also significantly increased. The S5 was moderately contaminated in winter, and the S2 was

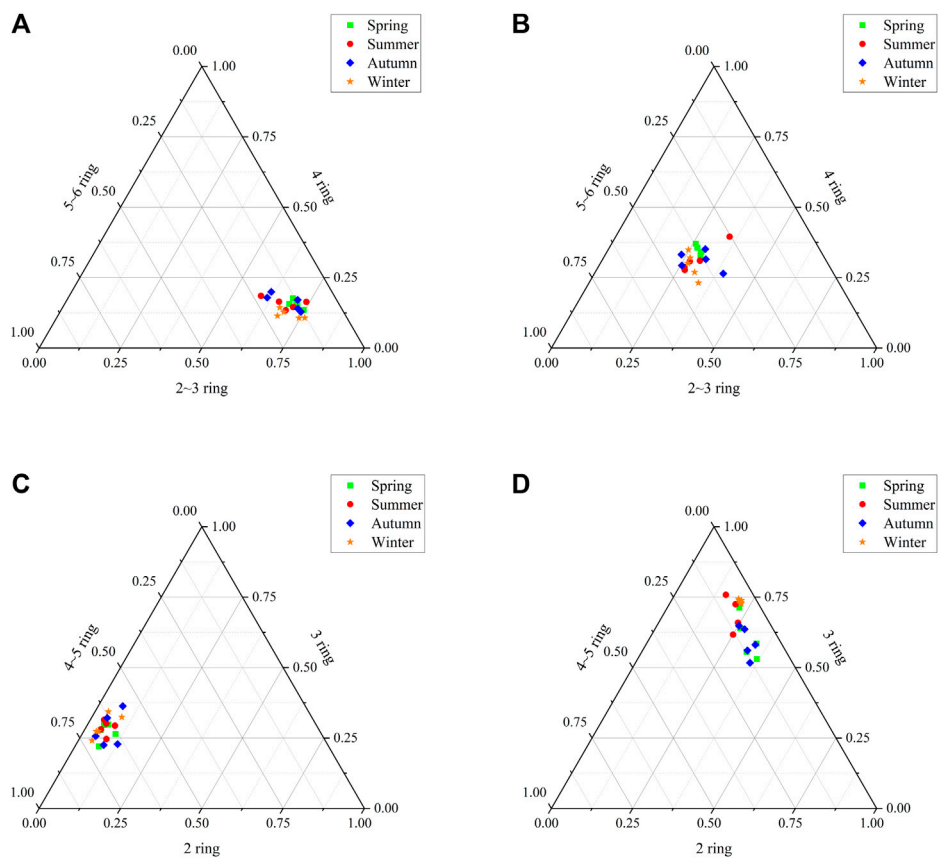


FIGURE 3 Triangle diagram of different kinds of PAHs for the seasonal distribution [Seasonal distribution of low and high ring of total PAHs (A); Seasonal distribution of 2–3, 4 and 5–6 ring of p-PAHs (B); Seasonal distribution of 2, 3 and 4–5 ring of p-PAHs (C); Seasonal distribution of 2, 3 and 4–5 ring of a-PAHs (D)].

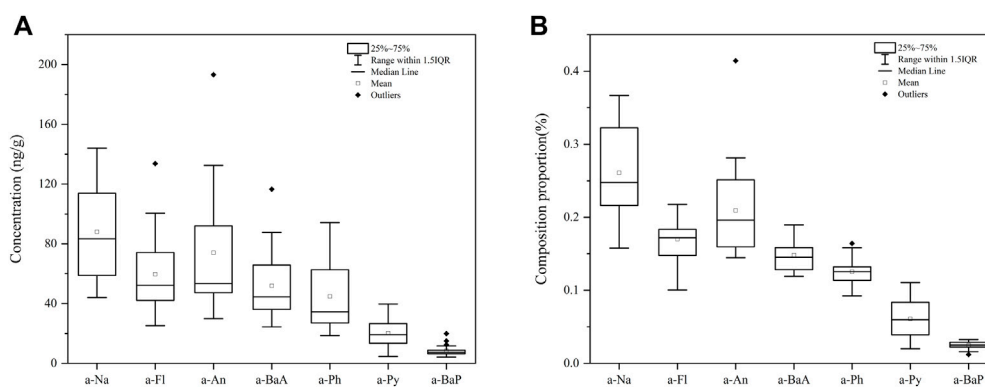


FIGURE 4 Box plot of a-PAHs homolog [concentration (A); proportion (B)].

TABLE 5 Toxic equivalent factors (TEFs), and BaP equivalent concentration (BaP_{eq}).

PAHs	TEF	Sites (1–5) (ng/g)	TEQ _{BaP}	Percentage (%)
Nap	0.001	49.970	0.050	0.03
Acy	0.001	0.000	0.000	0.00
Ace	0.001	0.000	0.000	0.00
Flu	0.001	66.155	0.066	0.03
Phe	0.001	74.673	0.075	0.04
Ant	0.010	67.928	0.679	0.34
Fla	0.001	80.055	0.080	0.04
Pyr	0.001	79.575	0.080	0.04
BaA	0.100	60.190	6.019	3.02
Chr	0.010	60.268	0.603	0.30
BbF	0.100	96.443	9.644	4.84
BkF	0.100	42.583	4.258	2.14
BaP	1.000	62.348	62.348	31.27
DaA	1.000	37.815	37.815	18.96
InP	0.100	45.615	4.562	2.29
BgP	0.010	62.815	0.628	0.32
C ₁₋₃ Nap	0.001	440.203	0.440	0.22
C ₁₋₂ Flu	0.001	297.895	0.298	0.15
C ₁₋₃ Ant	0.010	343.781	3.438	1.72
C ₁₋₃ BaA	0.100	259.143	25.914	13.00
C ₁₋₃ Phe	0.001	223.978	0.224	0.11
C ₁ Pyr	0.001	100.988	0.101	0.05
C ₁ BaP	1.000	42.088	42.088	21.11
∑p-PAHs		886.430	126.906	63.64
∑a-PAHs		1708.073	72.503	36.36
∑PACs		2594.503	199.409	100.00

non-pollution in summer and autumn, and the rest of the sample sites were all weakly polluted (Figure 5C). As seen from the analysis of total PAH concentrations, PAHs of all soil samples were above the level of weak contamination. Except for the S1 in summer, S1 and S5 samples of other sites and seasons were moderately contaminated (Figure 5A).

The equivalent concentration factor of a-PAHs was calculated based on p-PAHs (Chen et al., 2016). The toxicity equivalent concentration results showed that (Table 5): the maximum concentration of p-PAHs was BbF (96.44 ng/g); the minima were Acy and Ace; the maximum concentration of a-PAHs was C₁₋₃ Nap (440.20 ng/g); the minimum was C₁-BaP (42.09 ng/g). The evaluation results showed that BaP with a maximum toxic equivalent of 62.35 ng/g, C₁-BaP (42.09 ng/g), DaA (37.82 g/g) and C₁₋₃ BaA (26.91 ng/g) were the most important 4 types of PAHs with high toxicity risk. The risk value of ∑p-PAHs accounted for 63.64%, and it was the most important toxic risky PAHs in the soil of the karst coal mining area. As seen from the analysis of monomers and homologs, BaP and C₁-BaP contributed 52.38% of the toxicity risk, which were the most important toxic risky substances. It was worth noting

that both DaA and C₁₋₃ BaA toxicity risk accounted for more than 10%, which were also the main types of PAHs that affect the regional ecological risk. In the cultivated soil S3 and S4, a certain content of BaP may cause the enrichment of plants, which were transmitted in the food chain and caused certain toxicity risks to the local residents.

Discussion

Coal mining and consumption were the main sources of PAHs in soil. The average concentration of p-PAHs in the soil of karst coal mining areas was 177.29 ng/g. Shang et al. (2019) showed that the average concentration of p-PAHs in Chinese surface soil was 1217 ng/g, and the average content in Guizhou province was 117.8 ng/g. Compared with other chemical areas in China (Table 6), the pollution concentration of PAHs in the coal mining area of Guizhou province was at a low level. Compared with the PAHs pollution concentration in other regions of Guizhou province, the total concentration of PAHs in this study was at a moderate level, but was significantly lower than

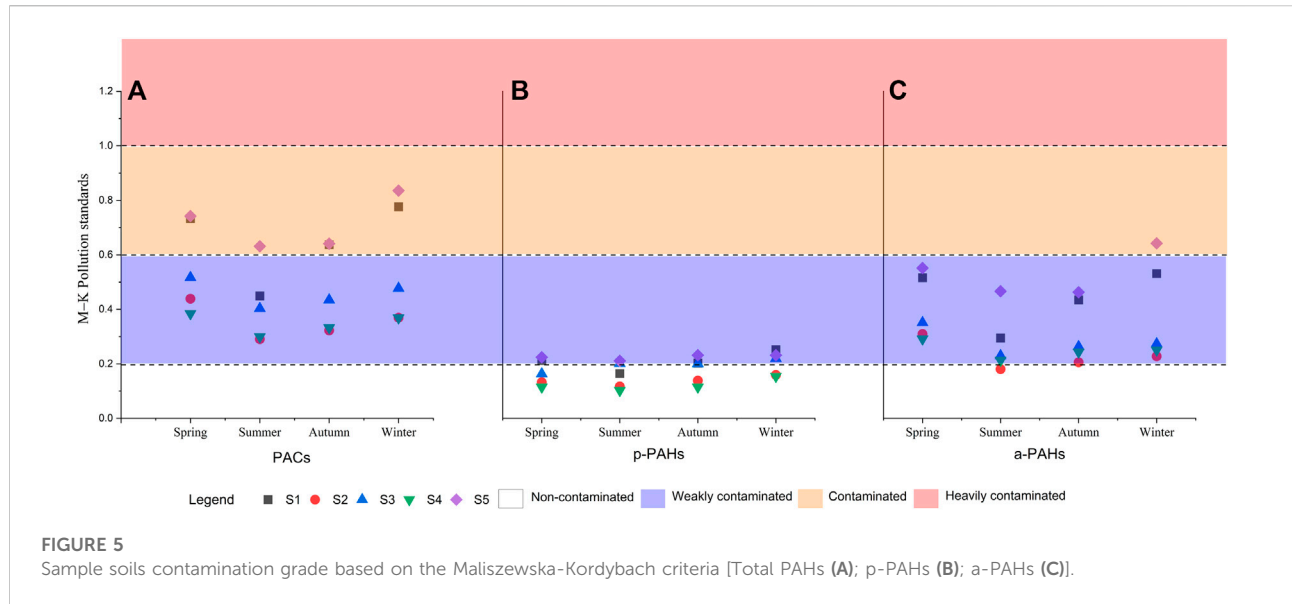


TABLE 6 Concentrations of PAHs in surface soils from different areas in China.

Study area	PAHs	Minimum	Maximum	Middle	Average	References	Samples time
Surface soil, China	16	ND	65500	381.9	1214	Shang et al. (2019)	1999–2018
Surface soil, China	16	9.90	5910	159	377	Zhao et al. (2015)	2015
Agricultural soil, China	16	ND	27580	ND	772	Sun et al. (2018)	2015
Agricultural top-soil,	16	277.79	3217.20	ND	1023	Liu et al. (2016)	2013
Urban soil, China	16	92	4733	ND	ND	Han et al. (2019)	2001–2017
Urban soil, China	16	30.1	23300	661	584	Ma et al. (2015)	2004–2013
Rural soil, China	16	3.7	6250	147	148	Ma et al. (2015)	2004–2013
Tangshan mining area, Hebei	16	115.30	1042.31	349.17	486.37	Jia et al. (2017).	ND
Yangtze River Delta Chemical Industry Park	19	16.3	4694	ND	688	Jia et al. (2021)	2019
Heshan coal district, Guangxi GGuangxi,China	16	79.56	4256.96	ND	1280.12	Huang et al. (2016)	2013
Coal mine district of Lu ling, Anhui	28	350	6210	ND	1690	Liu, (2014)	2010
Ningdong Chemical Industry District, Ningxia	16	ND	123120	ND	10190	Yang et al. (2020)	ND
Niangziguan karst catchment, Shanxi ,Niangziguan	16	47.13	705.3	194.4	259.96	Li et al. (2019)	ND
Suburb of Guiyang, Guizhou	16	61	511	339	281.8	Hu et al. (2006)	ND
Urban area of Guiyang, Guizhou	16	247	1560	692	663	Hu et al. (2006)	ND
Zunyi, Guizhou	16	0.8	251	ND	36.48	Zhang et al. (2009)	2008
Top-soil of Guiyang, Guizhou	16	10.02	1708.86	99.98	139.14	Zhang et al. (2021)	ND
Bijie, Guizhou	16	196	11592	780	1500	Chen et al. (2016)	2014–2015
Power plants in Bijie, Guizhou	16	200	12200	5350	4866	Zhang et al. (2021)	ND
Qiannan, Guizhou	16	3.7	259.6	ND	56.8	Lin et al. (2015)	2010
Coal mine district of Hezhang county, Guizhou	16	136.67	224.66	196.04	177.29	This study	2021
Coal mine district of Hezhang county, Guizhou	21	249.21	530.72	279.48	346.87	This study	2021

Note: ND means no data available in reference.

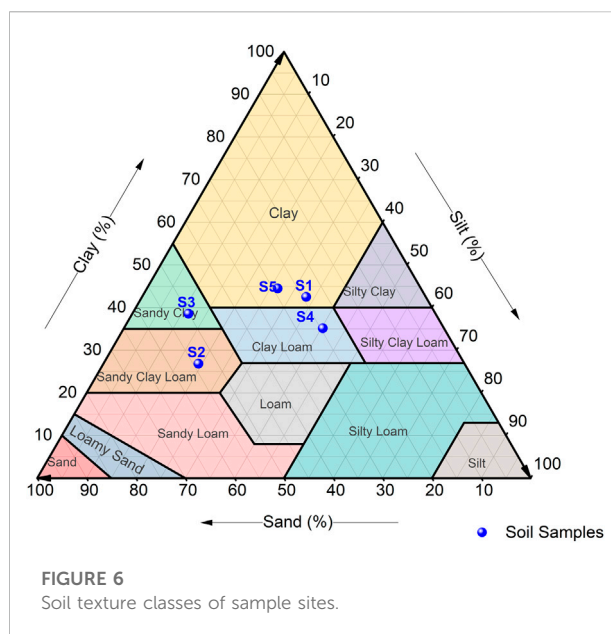
the regional pollution concentration of PAHs in Guizhou province coal power plants (4866 ng/g on average). The concentration in the karst area soil was at a moderate level,

which may be because coal was the main energy consumption patterns in the southwest karst area. Most of the coal consumption was at a low grade in northwest Guizhou

province, and the emission of PAHs from coal was significantly higher than that from high grade anthracite. Geng et al. (2014) believed that the overall emission coefficient of Guizhou province anthracite was 129.47 mg/kg, which was significantly higher than that of anthracite in other parts of China. Therefore, the accumulation of PAHs in the soil of Guizhou province coal mining areas may be derived from coal combustion and the emission of lithogenic PAHs during coal mining. In addition, the southwest karst area with high altitude, humid air, relatively closed terrain, and short illumination time hindered the diffusion of PAHs in the atmosphere, thereby increasing the concentration of PAHs in the soil matrix. The author's previous research showed that the karst soil with calcium-enriched characteristics might reduce the adsorption of PAHs. The main reason was that, in a complex karst environment, the soil inorganic ions repeatedly dissolve and precipitate, and occupied the high-energy sites for soil adsorption of PAHs, and filled soil pores. As a result, the PAHs entering the soil in karst areas may further migrate into groundwater or other environmental substrates, thus increasing the risk of environmental toxicity (An et al., 2021; An et al., 2022).

Soil organic matter, organic carbon, pH, particle composition, and soil microstructure are all factors to affect the occurrence state of PAHs. Many studies have shown that SOM was the key component for the sorption of organic pollutants by providing highly active combination sites, which was the key component for the adsorption and desorption of PAHs. It was believed that the PAHs desorption fractions and fast desorption rate constants of soils decreased with SOM increase (Li et al., 2007). Luo et al. (2012) illustrated that the fast-migrating components of PAHs in soil were directly related to organic carbon and the distribution of mesopores and micropores in soil. Ukalska-Jaruga et al. (2019) pointed out that different types of soil organic matter significantly affected the availability and durability of PAHs, and soil organic matter components of FA and HA were unstable components of organic matter, which had a significant positive correlation with the potential utilization of PAHs. HM was a stable organic matter with high hydrophobicity and poor degradability, which was the main factor affecting the durability of PAHs in soil. The sample site of S5 was rich in woodland and less affected by human activities.

The soil organic carbon content of S5 was significantly higher than other 4 sample sites. The total concentration of PAHs, the concentration of p-PAHs and a-PAHs of S5 was significantly higher than other 4 sample sites, which showed that PAHs concentration in the soil of the karst rocky desertification area was mainly controlled by soil organic carbon. High-ring (4-ring and 5–6-ring) p-PAHs and a-PAHs were more enriched for the sample sites of S5 and S3 with higher organic carbon content, indicating that high ring PAHs were more likely to bond with colloids such as soil organic matter and had greater migration difficulty in soil, which were consistent with previous findings



(Łyszczarz et al., 2021). At the same time, soil type was also an important factor to affect the environmental migration of PAHs. In this study, the soils of the S1 and S5 belonged to the clay soil type (Figure 6), which had a large sorption capacity for PAHs. The concentration of total PAHs in the study area had a good positive correlation with the soil clay content (Figure 7) ($R^2 = 0.88$). This was consistent with the findings of Luo et al. (2008) found that PAHs were mainly enriched in soil clay components. Pearson correlation analysis indicated that the total concentration of PAHs in soil was not only correlated with soil organic carbon and clay, but also had a significant positive correlation with the total calcium content of soil (Figure 7). Some studies pointed out that the higher the content of water-soluble calcium ions was in the soil, the greater the desorption components of PAHs were (An et al., 2022). The complex environmental conditions of karst may change the existing form of calcium ions in the soil, thus affecting the occurrence state of PAHs. Soil calcium can be divided into five forms: water-soluble calcium, exchangeable calcium, acid-soluble calcium, organically bound calcium and residual calcium. Soil calcium may also be an important driver of karst rocky desertification (Tang et al., 2019). The author believed that high calcium ions in karst soil might affect the occurrence and environmental migration of PAHs from two aspects: on the one hand, calcium ions affected the adsorption and desorption environmental conditions of PAHs, such as the cation exchange capacity; on the other hand, calcium ions was chemically changed in the complex karst environment, by forming inorganic precipitation or mineral polymer to affect the specific surface area of soil and its organic matter, reduce the high energy site of adsorption of PAHs, and the adsorption pores

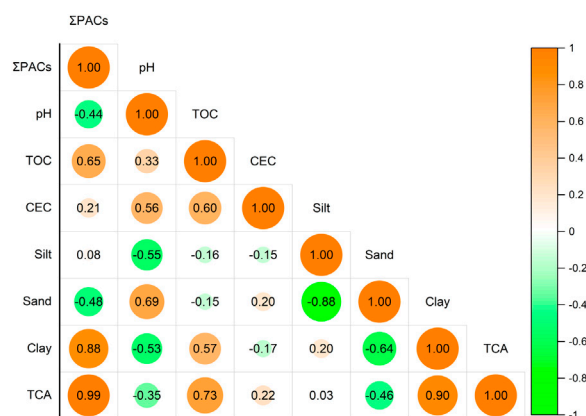


FIGURE 7
Correlation analysis of ΣPAHs concentration and soil properties.

(An et al., 2021). The role of various forms of calcium in the environmental transport of PAHs has not been systematically reported. Therefore, the effects of different calcium forms on PAHs carry great significance for karst soil management and remediation, and more in-depth studies are needed.

The natural environmental conditions in the karst rocky desertification area were complex, and the alternation of dry and wet, freeze-thaw cycles, rainfall leaching, and temperature fluctuations may change the occurrence state of PAHs in the regional soil and affect their migration. Seasonal alternation, temperature, rainfall, and large fluctuations in coal combustion can significantly affect the pollution concentration of PAHs in karst soils. Studies found that soil samples of PAHs concentration were higher in winter and spring than in summer and autumn, mainly due to the excessive coal combustion and the higher concentration of PAHs in the air in winter. In the karst mountain area, the temperature was relatively low in spring, and the amount of coal combustion was also high. In addition, there was continuous light rain before sampling in spring, making a large number of solid particles adsorb PAHs in the air and settle on the soil surface. Meijer et al. (2003) believed that the main factors affecting the distribution of PAHs between soil and atmosphere were soil characteristics, PAHs type and concentration, and air temperature. The concentration of PAHs in the soil was lower in summer, mainly because the amount of coal combustion was reduced and the temperature was high enough in summer, which made PAHs with higher volatility tend to re-volatilize in the atmosphere. At the same time, after the leaching of heavy rain, the vertical migration of PAHs concentration in soil was strengthened, which affected the PAHs concentration in the surface soil. It was worth

noting that a-PAHs have greater concentration reduction than p-PAHs during rainfall (the average soil concentration of p-PAHs reduced by 5.98% in summer than spring, and the average concentration of a-PAHs reduced by 31.48% in summer than spring). In particular, the low-ring a-PAHs had the most obvious reduction, which showed that the a-PAHs were greater environmental migration characteristics, so the environmental risk impact was more obvious, which may be closely related to the properties of the a-PAHs. Studies had shown that the physicochemical properties of a-PAHs (such as solubility, partition coefficient, etc.) were significantly different from those of p-PAHs (Kang et al., 2016). The solubility of 9-methylanthracene was 0.39 mg/L, which was significantly higher than the 0.044 mg/L of anthracene, (Kwon and Kwon, 2012), which related to the position and symmetrical structure of the alkylated substituent (Pinal 2004). Rainfall can significantly alter soil water content, affecting SOM's ability to adsorb PAHs. Schneckenburger and Thiele. (2020) pointed out that SOM matrix rigidity varied with prehydration status; the water content of SOM could change the soil matrix rigidity, which affected the adsorption and desorption of PAHs, altering the environmental migration of PAHs and their homologs. The complex karst environmental conditions such as the dry-wet cycle and freeze-thaw cycle also affect the migration behavior of PAHs in soil. Dry-wet cycles and freeze-thaw effects can alter the soil structure and affect the form of mineral ions in the soil, thereby changing the occurrence state of PAHs. Studies have shown that multiple freeze-thaw cycles of karst soils would reduce the soil's ability to desorb PAHs, making more PAHs turn into isolated states (An et al., 2021).

Risk assessments of PAHs in soil tend to focus on the 16 kinds of p-PAHs. However, a-PAHs were more environmentally toxic (Zhang et al., 2020; Huang et al., 2021), which may be related to the structure (Bay region) of a-PAHs (Baird et al., 2007). According to the air quality standards published in Canada, the BaP equivalent toxicity of dimethyl substituted BaA was 100 times that of parent BaA (Atmospheric quality standards and criteria, 2021). Without considering the concentration of a-PAHs, the S1 and S5 belonged to slightly polluted soil, while the concentration of a-PAHs in the five sampling sites was above the threshold of 200 ng/g of slight soil pollution (Maliszewska-Kordybach 1996). In general, the coal mining area soils and forest soils in the karst mining areas of southwest China were moderately polluted, while the cultivated soils were slightly polluted. Although the total concentration of PAHs was not equal to the bioavailability concentration of PAHs, the environmental risks of PAHs still should be paid more concern from local governments and residents. Therefore, to assess the risk of PAHs in soil, more consideration should be given to PAH substitutions such as the alkylated and nitro functional group to truly and accurately calculate the environmental risk of PAHs.

Conclusion

The concentration of p-PAHs and a-PAHs in surface soils of karst coal mining areas in Guizhou province, China displayed significantly different spatial and temporal distribution characteristics. The a-PAHs in the soil of the coal mining area had significantly higher pollution concentration than p-PAHs. The average concentration of p-PAHs and a-PAHs were 177.29 ± 37.36 ng/g and 346.87 ± 104.91 ng/g, respectively. The pollutant concentrations of PAHs exhibited a seasonal tendency with winter > spring > autumn > summer. The two types of PAHs in the study area were both affected by environmental events such as seasonal rainfall, and the a-PAHs were more greatly affected by rainfall than the p-PAHs, which closely related to the soil properties of the sampling site and the properties of a-PAHs. The soils of coal mining area and forest soils were moderately polluted, while cultivated soil and abandoned soil were slightly polluted. The toxicity results showed that p-BaP, C₁-BaP, DaA and C₁₋₃ BaA were the most important four types of toxic PAHs. Pearson correlation analysis illustrated that soil calcium content in the karst area was also an important factor affecting the distribution of regional PAHs. The environmental migration and fate of PAHs under different forms of calcium in karst soils require to be more deeply and systematically study in future. The research is helpful for guiding significance for the control and restoration of soil PAH in the karst area of southwest China with fragile ecology and complex environment.

Data availability statement

The original contributions presented in the study are included in the article/Supplementary Materials, further inquiries can be directed to the corresponding author.

Author contributions

XA: Conceptualization, Methodology, Validation, Resources, Data Curation, and Writing-Original draft preparation. WL: Supervision, Investigation, Writing-reviewing and Editing. JL: Investigation, Data Curation, and Software. XD: Visualization, Software, and Formal analysis. MA: Writing-reviewing, Editing, and Data curation.

Funding

This work was supported the National Natural Science Foundation of China (No. 41761091); The First-class Discipline Group of Geography of Guizhou Province (No. [2019]125); Guizhou Education Department Youth Science and Technology Talents Growth Project, China (KY[2022] 001); Fundamental Scientific Research Funds of Guiyang University, China (GYU-KY-[2022]); The Joint Foundation of Guizhou Province (LH[2017]7348); The Doctor Foundation of Guizhou Normal University (GZNUD [2017]10).

Acknowledgments

We thank the editor and three anonymous reviewers for their valuable comments on the manuscript. The authors thank the support of Open Project Fund of school of Mountain Research of Guizhou Education University.

Conflict of interest

The authors declare that the research was conducted in the absence of any commercial or financial relationships that could be construed as a potential conflict of interest.

Publisher's note

All claims expressed in this article are solely those of the authors and do not necessarily represent those of their affiliated organizations, or those of the publisher, the editors and the reviewers. Any product that may be evaluated in this article, or claim that may be made by its manufacturer, is not guaranteed or endorsed by the publisher.

References

- An, X. J., Li, W., Di, X. Y., and Xiao, B. H. (2021). Effects of supergene geochemical processes on desorption and bioavailability of polycyclic aromatic hydrocarbons in soil of karst area. *Environ. Pollut. Bioavailab.* 33 (1), 402–414. doi:10.1080/26395940.2021.1990799
- An, X. J., Li, W., Lan, J. C., and Di, X. Y. (2022). Study on the desorption behavior and bioavailability of polycyclic aromatic hydrocarbons in different rocky desertification soils. *Pol. J. Environ. Stud.* 31 (5), 1–15. doi:10.15244/pjoes/149999
- Andersson, J. T., and Achten, C. (2015). Time to say goodbye to the 16 EPA PAHs? Toward an up-to-date use of PACs for environmental purposes. *Polycycl. Aromat. Compd.* 35 (2–4), 330–354. doi:10.1080/10406638.2014.991042
- Atmospheric quality standards and criteria (2021). *Gouvernement du Québec*. Québec: Canada.
- Baird, S. J., Bailey, E. A., and Vorhees, D. J. (2007). Evaluating human risk from exposure to alkylated PAHs in an aquatic system. *Hum. Ecol. Risk Assess. An Int. J.* 13 (2), 322–338. doi:10.1080/10807030701226277
- Chen, F., Wang, C. C., Zhang, L. J., Wei, X. H., and Wang, Q. (2016). Characteristics, sources apportionment and risk assessment of polycyclic aromatic hydrocarbons in agricultural soils from zinc smelting area, Guizhou Province. *Acta Sci. Circumstantiae* 37 (04), 1515–1523. (In Chinese). doi:10.13671/j.hjkxb.2016.0325
- Geng, C. M., Chen, J. H., Yang, X. H., Ren, L. H., Yin, B. H., Liu, X. Y., et al. (2014). Emission factors of polycyclic aromatic hydrocarbons from domestic coal combustion in China. *J. Environ. Sci.* 26 (1), 160–166. doi:10.1016/S1001-0742(13)60393-9
- Golzadeh, N., Barst, B. D., Baker, J. M., Auger, J. C., and McKinney, M. A. (2021). Alkylated polycyclic aromatic hydrocarbons are the largest contributor to polycyclic aromatic compound concentrations in traditional foods of the Bigstone Cree Nation in Alberta, Canada. *Environ. Pollut.* 275, 116625. doi:10.1016/j.envpol.2021.116625
- Han, J., Liang, Y. S., Zhao, B., Wang, Y., Xing, F. T., and Qin, L. B. (2019). Polycyclic aromatic hydrocarbon (PAHs) geographical distribution in China and their source, risk assessment analysis. *Environ. Pollut.* 251, 312–327. doi:10.1016/j.envpol.2019.05.022
- Hellou, J., Mackay, D., and Banoub, J. (1999). Levels, persistence and bioavailability of organic contaminants present in marine harbor sediments impacted by raw sewage. *Chemosphere* 38 (2), 457–473. doi:10.1016/S0045-6535(98)00184-2
- Hu, J., Zhang, G., and Lui, C. Q. (2006). Pilot study of polycyclic aromatic hydrocarbons in surface soils of Guiyang city, People's Republic of China. *Bull. Environ. Contam. Toxicol.* 76 (1), 80–89. doi:10.1007/s00128-005-0892-8
- Huang, H. F., Xing, X. L., Zhang, Z. Z., Qi, S. H., Yang, D., Yuen, D. A., et al. (2016). Polycyclic aromatic hydrocarbons (PAHs) in multimedia environment of heshan coal district, guangxi: Distribution, source diagnosis and health risk assessment. *Environ. Geochem. Health* 38 (5), 1169–1181. doi:10.1007/s10653-015-9781-1
- Huang, Q., Zhu, Y. X., Wu, F., and Zhang, Y. (2021). Parent and alkylated polycyclic aromatic hydrocarbons in surface sediments of mangrove wetlands across Taiwan Strait, China: Characteristics, sources and ecological risk assessment. *Chemosphere* 265, 129168. doi:10.1016/j.chemosphere.2020.129168
- Jia, H. B., Zhang, L. X., Li, Y., Zhang, X. N., Wang, X. M., Feng, S. D., et al. (2017). Concentration characteristics and sources apportionment of PAHs from the coal mining area soil. *J. Hebei Agric. Univ.* 40 (02), 24–31. (In Chinese). doi:10.13320/j.cnki.jauh.2017.0029
- Jia, T. Q., Guo, W., Xing, Y., Lei, R. R., Wu, X. L., Sun, S. R., et al. (2021). Spatial distributions and sources of PAHs in soil in chemical industry parks in the Yangtze River Delta, China. *Environ. Pollut.* 283, 117121. doi:10.1016/j.envpol.2021.117121
- Kang, H. J., Lee, S. Y., and Kwon, J. H. (2016). Physico-chemical properties and toxicity of alkylated polycyclic aromatic hydrocarbons. *J. Hazard. Mat.* 312, 200–207. doi:10.1016/j.jhazmat.2016.03.051
- Kang, H. J., Lee, S. Y., and Kwon, J. H. (2016). Physico-chemical properties and toxicity of alkylated polycyclic aromatic hydrocarbons. *J. Hazard. Mat.* 312, 200–207. doi:10.1016/j.jhazmat.2016.03.051
- Kwon, H. C., and Kwon, J. H. (2012). Measuring aqueous solubility in the presence of small cosolvent volume fractions by passive dosing. *Environ. Sci. Technol.* 46 (22), 12550–12556. doi:10.1021/es3035363
- Lan, J. C., Sun, Y. C., Xiao, S. Z., and Yuan, D. X. (2016). Polycyclic aromatic hydrocarbon contamination in a highly vulnerable underground river system in Chongqing, Southwest China. *J. Geochem. Explor.* 168, 65–71. doi:10.1016/j.gexplo.2016.05.013
- Lan, J. C., Sun, Y. C., and Yuan, D. X. (2018). Transport of polycyclic aromatic hydrocarbons in a highly vulnerable karst underground river system of southwest China. *Environ. Sci. Pollut. Res.* 25 (34), 34519–34530. doi:10.1007/s11356-018-3005-z
- Larson, E. B., and Mylroie, J. E. (2018). Diffuse versus conduit flow in coastal karst aquifers: The consequences of island area and perimeter relationships. *Geosciences* 8 (7), 268. doi:10.3390/geosciences8070268
- Li, C. C., Zhang, X., Gao, X. B., Qi, S. H., and Wang, Y. X. (2019). The potential environmental impact of PAHs on soil and water resources in air deposited coal refuse sites in Niangziguan Karst Catchment, Northern China. *Int. J. Environ. Res. Public Health* 16 (8), 1368. doi:10.3390/ijerph16081368
- Li, J. G., Sun, H. W., and Zhang, Y. (2007). Desorption of pyrene from freshly-amended and aged soils and its relationship to bioaccumulation in earthworms. *Soil Sediment Contam. An Int. J.* 16 (1), 79–87. doi:10.1080/15320380601079665
- Liang, M., Liang, Y. C., Liang, H. D., Rao, Z., and Cheng, H. F. (2018). Polycyclic aromatic hydrocarbons in soil of the backfilled region in the Wuda coal fire area, Inner Mongolia, China. *Ecotoxicol. Environ. Saf.* 165, 434–439. doi:10.1016/j.ecoenv.2018.08.065
- Lin, Y., Fang, Z. Q., Wang, Z. K., and Luo, Y. C. (2015). Pollution characteristics of polycyclic aromatic hydrocarbon in topsoil of Guizhou Qiannan District. *Guizhou Agric. Sci.* 43 (1), 159–161. (In Chinese).
- Lin, Y. X., Deng, W., Li, S. Y., Li, J. F., Wang, G. G., Zhang, D. H., et al. (2017). Congener profiles, distribution, sources and ecological risk of parent and alkyl-PAHs in surface sediments of Southern Yellow Sea, China. *Sci. Total Environ.* 580, 1309–1317. doi:10.1016/j.scitotenv.2016.12.094
- Liu, J. J. (2014). *Geochemical cycling of hydrocarbon compounds in soil of typical coal mine district*. Hefei: University of Science and Technology of China.
- Liu, J. L., Zhang, S. Y., Jia, J. L., Lou, M. J., Li, X., Zhao, S. W., et al. (2022). Distribution and source apportionment of polycyclic aromatic hydrocarbons in soils at different distances and depths around three power plants in bijie, Guizhou province. *Polycycl. Aromat. Compd.*, 1–12. doi:10.1080/10406638.2022.2039232
- Liu, M. X., Yang, Y. Y., Yun, X. Y., Zhang, M. M., and Wang, J. (2016). Occurrence, sources, and cancer risk of polycyclic aromatic hydrocarbons and polychlorinated biphenyls in agricultural soils from the Three Gorges Dam region, China. *J. Soil Water Conserv.* 71 (4), 327–334. doi:10.2489/jswc.71.4.327
- Luo, L., Lin, S., Huang, H. L., and Zhang, S. Z. (2012). Relationships between aging of PAHs and soil properties. *Environ. Pollut.* 170, 177–182. doi:10.1016/j.envpol.2012.07.003
- Luo, L., Zhang, S. Z., and Ma, Y. B. (2008). Evaluation of impacts of soil fractions on phenanthrene sorption. *Chemosphere* 72 (6), 891–896. doi:10.1016/j.chemosphere.2008.03.051
- Łyszczarz, S., Lasota, J., Szuszkiewicz, M. M., and Błońska, E. (2021). Soil texture as a key driver of polycyclic aromatic hydrocarbons (PAHs) distribution in forest topsoils. *Sci. Rep.* 11 (1), 14708–14711. doi:10.1038/s41598-021-94299-x
- Ma, W. L., Liu, L. Y., Tian, C. G., Qi, H., Jia, H. L., Song, W. W., et al. (2015). Polycyclic aromatic hydrocarbons in Chinese surface soil: Occurrence and distribution. *Environ. Sci. Pollut. Res.* 22 (6), 4190–4200. doi:10.1007/s11356-014-3648-3
- Maliszewska-Kordybach, B. (1996). Polycyclic aromatic hydrocarbons in agricultural soils in Poland: Preliminary proposals for criteria to evaluate the level of soil contamination. *Appl. Geochem.* 11 (1–2), 121–127. doi:10.1016/0883-2927(95)00076-3
- Meijer, S. N., Shoeib, M., Jantunen, L. M. M., Jones, K. C., and Harner, T. (2003). Air–soil exchange of organochlorine pesticides in agricultural soils. 1. Field measurements using a novel *in situ* sampling device. *Environ. Sci. Technol.* 37 (7), 1292–1299. doi:10.1021/es020540r
- Pinal, R. (2004). Effect of molecular symmetry on melting temperature and solubility. *Org. Biomol. Chem.* 2 (18), 2692–2699. doi:10.1039/B407105K
- Qian, Y. H., Wang, T., Hong, X. P., Luo, Z. G., and Liang, H. D. (2022). Quantitative method of alkyl polycyclic aromatic hydrocarbons in surface soils of coal mines. *J. Chin. Mass Spectrom. Soc.* 43 (02), 168–177. (In Chinese). doi:10.7538/zpxb.2021.0065
- Qian, Z., Mao, Y., Xiong, S., Peng, B., Liu, W., Liu, H. F., et al. (2020). Historical residues of organochlorine pesticides (OCPs) and polycyclic aromatic hydrocarbons (PAHs) in a flood sediment profile from the Longwang Cave in Yichang, China. *Ecotoxicol. Environ. Saf.* 196, 110542. doi:10.1016/j.ecoenv.2020.110542
- Schneckenburger, T., and Thiele-Bruhn, S. (2020). Sorption of PAHs and PAH derivatives in peat soil is affected by prehydration status: The role of SOM and sorbate properties. *J. Soils Sediments* 20 (10), 3644–3655. doi:10.1007/s11368-020-02695-z
- Shang, Q. B., Duan, Y. H., Xu, L. S., Duan, H. R., He, J. L., Cheng, R., et al. (2019). Spatial distribution and genesis of polycyclic aromatic hydrocarbons (PAHs) in the

- surface soil in China. *J. Ecol. Rural Environ.* 35 (09), 917–924. doi:10.19741/j.issn.1673-4831.2018.0866
- Sun, J. T., Pan, L. L., Tsang, D. C. W., Zhan, Y., Zhu, L. Z., and Li, X. D. (2018). Organic contamination and remediation in the agricultural soils of China: A critical review. *Sci. Total Environ.* 615, 724–740. doi:10.1016/j.scitotenv.2017.09.271
- Tang, J., Tang, X. X., Qin, Y. M., He, Q. S., Yi, Y., and Ji, Z. L. (2019). Karst rocky desertification progress: Soil calcium as a possible driving force. *Sci. Total Environ.* 649, 1250–1259. doi:10.1016/j.scitotenv.2018.08.242
- Ukalska-Jaruga, A., Smreczak, B., and Klimkiewicz-Pawlas, A. (2019). Soil organic matter composition as a factor affecting the accumulation of polycyclic aromatic hydrocarbons. *J. Soils Sediments* 19 (4), 1890–1900. doi:10.1007/s11368-018-2214-x
- Wei, C., Bandowe, B. A. M., Han, Y. M., Cao, J. J., Zhan, C. L., and Wilcke, W. (2015). Polycyclic aromatic hydrocarbons (PAHs) and their derivatives (alkyl-PAHs, oxygenated-PAHs, nitrated-PAHs and azaarenes) in urban road dusts from Xi'an, Central China. *Chemosphere* 134, 512–520. doi:10.1016/j.chemosphere.2014.11.052
- Xu, S. S., Liu, W. X., and Tao, S. (2006). Emission of polycyclic aromatic hydrocarbons in China. *Environ. Sci. Technol.* 40 (3), 702–708. doi:10.1021/es0517062
- Yan, Y. J., Dai, Q. H., Jin, L., and Wang, X. D. (2019). Geometric morphology and soil properties of shallow karst fissures in an area of karst rocky desertification in SW China. *Catena* 174, 48–58. doi:10.1016/j.catena.2018.10.042
- Yang, F., Luo, H. X., Zhong, Y. X., Wang, Y. Q., and Bai, Y. R. (2020). Spatial distribution characteristics, source apportionment, and risk assessment of topsoil PAHs in the core area of the ningdong energy and chemical industry base. *Environ. Sci.* 42 (05), 2490–2501. (In Chinese). doi:10.13227/j.hjkk.202009096
- Ye, X. C., Yang, P. H., and Zhang, Q. (2015). Hydrogeochemical processes and vulnerability of a typical karst underground river system, southwest China. *Geochem. J.* 49 (3), 259–269. doi:10.2343/geochemj.2.0354
- Zhang, G. L., Lan, T. T., Yang, G. Q., Li, J. M., and Zhang, K. K. (2021). Contamination, spatial distribution, and source contribution of persistent organic pollutants in the soil of Guiyang city, China: A case study. *Environ. Geochem. Health*, 1–14. doi:10.1007/s10653-021-01089-5
- Zhang, M. S., Teng, M. D., Li, Q. H., Lin, Y., and Ye, F. (2009). Distribution characteristics of polycyclic aromatic hydrocarbons in top soils in zunyi, Guizhou province. *J. Jiangxi Normal Univ. Nat. Sci. Ed.* 33 (6), 716–720. DOI:(In Chinese). doi:10.16357/j.cnki.issn1000-5862.2009.06.019
- Zhang, Y., Shen, Z. X., Sun, J., Zhang, L. M., Zhang, B., Zhang, T., et al. (2020). Parent, alkylated, oxygenated and nitro polycyclic aromatic hydrocarbons from raw coal chunks and clean coal combustion: Emission factors, source profiles, and health risks. *Sci. Total Environ.* 721, 137696. doi:10.1016/j.scitotenv.2020.137696
- Zhang, Y., Shen, Z. X., Sun, J., Zhang, L. M., Zhang, B., Zou, H. J., et al. (2021). Parent, alkylated, oxygenated and nitrated polycyclic aromatic hydrocarbons in PM_{2.5} emitted from residential biomass burning and coal combustion: A novel database of 14 heating scenarios. *Environ. Pollut.* 268, 115881. doi:10.1016/j.envpol.2020.115881
- Zhang, Y. X., Tao, S., Cao, J., and Coveney, R. M. (2007). Emission of polycyclic aromatic hydrocarbons in China by county. *Environ. Sci. Technol.* 41 (3), 683–687. doi:10.1021/es061545h
- Zhao, X., Qiu, H. R., Zhao, Y. L., Shen, J. M., Chen, Z. L., and Chen, J. X. (2015). Distribution of polycyclic aromatic hydrocarbons in surface water from the upper reach of the Yellow River, Northwestern China. *Environ. Sci. Pollut. Res.* 22 (9), 6950–6956. doi:10.1007/s11356-014-3846-z
- Zhu, Y. X., Liang, B., Xia, W. W., Gao, M., Zheng, H. J., Chen, J., et al. (2022). Assessing potential risks of aquatic polycyclic aromatic compounds via multiple approaches: A case study in jialing and yangtze rivers in downtown chongqing, China. *Environ. Pollut.* 294, 118620. doi:10.1016/j.envpol.2021.118620